Structure of the Active Sites on H 3 PO 4 /ZrO 2 Catalysts for Dimethyl Carbonate Synthesis from Methanol and Carbon Dioxide

ARTICLE *in* THE JOURNAL OF PHYSICAL CHEMISTRY B · NOVEMBER 2001

Impact Factor: 3.3 · DOI: 10.1021/jp0121522

4 AUTHORS, INCLUDING:

Mohammad Asadullah
Universiti Teknologi MARA
84 PUBLICATIONS **2,099** CITATIONS
SEE PROFILE

Kaoru Fujimoto
Kitakyushu University
366 PUBLICATIONS **6,977** CITATIONS
SEE PROFILE

Structure of the Active Sites on H_3PO_4/ZrO_2 Catalysts for Dimethyl Carbonate Synthesis from Methanol and Carbon Dioxide

Yoshiki Ikeda, Mohammad Asadullah, Kaoru Fujimoto, and Keiichi Tomishige*

Department of Applied Chemistry, School of Engineering, The University of Tokyo, 7-3-1 Hongo, Bunkyo-ku, Tokyo 113-8656, Japan

Received: June 6, 2001; In Final Form: August 5, 2001

The catalytic properties of H_3PO_4/ZrO_2 catalysts for dimethyl carbonate (DMC) synthesis from CH_3OH and CO_2 were investigated. The modification of ZrO_2 with H_3PO_4 promoted the activity for selective DMC formation. The characterization of H_3PO_4/ZrO_2 catalysts was performed by means of BET, XRD, ^{31}P MAS NMR, LRS, DRIFT, and NH_3-TPD. From the characterization results, it was determined that ZrO_2 had Lewis acid sites and did not have Brønsted acid sites. The presence of Brønsted acid sites as well as Lewis acid sites was observed on H_3PO_4/ZrO_2 (P/Zr = 0.05). The acidity of the Brønsted sites is weak, and the site's structure is a bridged OH. Furthermore, this Brønsted site is formed by the interaction between tetragonal Zr and P. In the reaction scheme of DMC formation, the Brønsted acid site can contribute to CH_3OH activation and to the enhancement of the catalytic activity.

Introduction

The development of CO_2-based methods for the synthesis of carbonic acid diesters is very attractive.[1] Dimethyl carbonate (DMC), the lowest homologue of this family, is drawing much attention as a safe, noncorrosive, and environmentally acceptable substitute for the carbonylating and methylating agents phosgene and dimethyl sulfate.[2] DMC can also be used as an octane booster in gasoline.[3] Furthermore, the addition of DMC to diesel fuel decreases the emission of particulate matter. If DMC were used as a fuel additive, a large scale-up of current world DMC production would be necessary.

Three methods of DMC production have been developed. The first is the stoichiometric reaction of methanol and phosgene in a concentrated sodium hydroxide solution.[4]

$$2CH_3OH + COCl_2 \rightarrow (CH_3O)_2CO + 2HCl$$

The second is the oxidative carbonylation of CH_3OH with carbon monoxide and oxygen, catalyzed by cuprous chloride in a slurry reaction system,[5−7] where the reaction proceeds in a redox cycle of copper ions as follows:

$$2CuCl + 2CH_3OH + {}^1/_2O_2 \rightarrow 2Cu(OCH_3)Cl + H_2O$$

$$2Cu(OCH_3)Cl + CO \rightarrow (CH_3O)_2CO + 2CuCl$$

The third is an excellent DMC synthesis process based on oxidative carbonylation using a palladium catalyst and a methyl nitrite promoter.[8]

$$CO + 2CH_3ONO \rightarrow (CH_3O)_2CO + 2NO$$

The methyl nitrite used in this process is synthesized by the following reaction, which proceeds at room temperature without any catalyst:

$$2CH_3OH + 2NO + {}^1/_2O_2 \rightarrow 2CH_3ONO + H_2O$$

Some of the other routes to DMC synthesis from CO_2 have recently been reported. The selective DMC synthesis via the reaction of supercritical CO_2 and trimethyl orthoacetate using the molecular catalyst $Bu_2Sn(OCH_3)_2$ has been reported.[9]

$$CH_3C(OCH_3)_3 + CO_2 \rightarrow (CH_3O)_2CO + CH_3COOCH_3$$

It is known that DMC can be synthesized directly from CH_3OH and CO_2 in the presence of dialkoxydibutyltin.[10] The reactions were carried out under pressure with CO_2. It is assumed that CO_2 is inserted into the Sn−O bond of $Bu_2Sn(OCH_3)_2$ followed by alcoholysis, yielding carbonate and $Bu_2Sn(OH)_2$. This species is again esterified by methanol so that the tin catalyst can be reused.

$$2CH_3OH + CO_2 \rightarrow (CH_3O)_2CO + H_2O$$

It has also been reported that DMC can be synthesized from CH_3OH and CO_2 in the presence of tin(IV) and titanium(IV) alkoxides and the metal acetates.[11] The water produced with DMC causes the deactivation of these alkoxide catalysts.

Recently, we have reported that DMC was selectively synthesized from CH_3OH and CO_2 using zirconia catalysts.[12] With some other catalysts, dimethyl ether (DME) was formed, where DMC was not detected at all.[12,13] It is characteristic that DME formation on ZrO_2 is below the detection limit. The amount of DMC formation showed the volcano-type dependence on the calcination temperature of zirconium hydroxide.[12,14] It was found that the DMC formation rate was strongly dependent on the acid−base bifunctional properties on ZrO_2.

We have also reported that the modification of ZrO_2 catalysts with phosphoric acid promoted activity for DMC synthesis with high selectivity and that the reactions proceeded at much lower temperatures with modified ZrO_2 catalysts than with the unmodified ZrO_2.[15] In this paper, we characterized phosphoric acid-modified ZrO_2 catalysts with various phosphoric acid

* Present address: Institute of Materials Science, University of Tsukuba, 1-1-1 Tennodai, Tsukuba, Ibaraki 305-8573, Japan. Tel and Fax: +81-298-53-5030. E-mail: tomi@tulip.sannnet.ac.jp.

10.1021/jp0121522 CCC: $20.00
Published on Web 10/05/2001

contents by means of Brunauer−Emmett−Teller (BET) surface area, X-ray diffraction (XRD), ^{31}P magic-angle spinning NMR spectroscopy (^{31}P MAS NMR), laser Raman spectroscopy (LRS), diffuse reflectance infrared Fourier transform (DRIFT), and ammonia temperature-programmed desorption (NH_3-TPD) in order to elucidate the promoting mechanism.

Experimental Methods

Catalyst Preparation. ZrO_2 was prepared by calcining a commercially available zirconium hydroxide ($ZrO_2 \cdot xH_2O$; Nacalai Tesque Inc.) at 673 K for 3 h in air. Phosphoric acid-modified ZrO_2 catalysts were prepared by impregnating $ZrO_2 \cdot xH_2O$ with an aqueous H_3PO_4 solution (Aldrich, 85 wt %). Water was removed by heating, and the sample was dried at 393 K for 10 h, followed by calcination at 673 K for 3 h in air. The calcination temperature of these catalysts was also optimized.[12−15] These catalysts are represented by H_3PO_4/ZrO_2. The content of H_3PO_4 is denoted as the molar ratio P/Zr in parentheses [e.g., H_3PO_4/ZrO_2 (P/Zr = 0.05)].

DMC Synthesis from CH_3OH and CO_2. The reaction was carried out in a stainless steel autoclave reactor with an inner volume of 70 mL. The standard procedure is as follows: 6.1 g of CH_3OH (192 mmol; Kanto Chemical, 99.8% min) and 0.5 g of the catalyst were placed in an autoclave, and then the reactor was purged with CO_2. A total of 8.8 g of CO_2 (200 mmol; Takachiho Trading Co. Ltd., 99.99%) was introduced, and the initial pressure was about 4 MPa at room temperature. The reactor was heated and magnetically stirred constantly during the reaction. The reaction was carried out at different temperatures (383−443 K) for 2 h. Products in both the gas and liquid phases were analyzed by gas chromatograph (GC) equipped with a flame ionization detector (FID) and a thermal conductivity detector (TCD). In the gas phase, no products were observed. CO was below the detection limit of the FID-GC equipped with a methanator. Under all of the reaction conditions shown in this paper, DMC was the only product, and DME was below the detection limit of the FID-GC.

Catalyst Characterization. BET surface area, XRD patterns, and LRS spectra of the catalysts were measured with a Gemini 2360 (Micromeritics, N_2 adsorption), a RINT-2400 (Rigaku, Cu Kα), and a LABRAM 1B (JOBIN-YBON, He−Ne laser), respectively. ^{31}P MAS NMR spectra were obtained at 121.65 MHz on a Fourier transform pulsed NMR spectrometer (JEOL JNM-CMX-300). The weight of each sample for ^{31}P MAS NMR was about 0.4 g. The spinning speed was 5.0 kHz. Proton decoupling and cross polarization were not employed. DRIFT spectra were obtained using a Magna 550 (Nicolet) with an MCT detector. An in-situ cell (Spectra-Tech) was used for high-temperature and high-pressure observations. Catalyst powder was placed in the sample cup in the cell. This cell was connected to the high-pressure gas flow system. Pretreatment was carried out in N_2 flow at 673 K for 0.5 h. CH_3OH (Kanto Chemical, 99.8% min) was introduced by the pulsed gas under atmospheric pressure at 443 K with N_2 as a carrier gas until the coverage reached the saturation level. Then, CO_2 (Takachiho Trading Co. Ltd., 99.99%) was introduced onto the CH_3OH-preadsorbed sample under atmospheric pressure, and CO_2 was pressurized stepwise to 5 MPa, where the sample temperature was kept at 443 K. Each spectrum was obtained 3 min after the introduction of CO_2 at each pressure. To obtain the profiles of NH_3-TPD, NH_3 (Takachiho Trading Co. Ltd., 99.999%) was introduced at 298 K by the same procedure as that of CH_3OH after the pretreatment. The sample was heated to 673 K. Each spectrum was obtained 10 min after the target temperature was reached.

TABLE 1. Dependence of DMC Formation and BET Surface Area of H_3PO_4/ZrO_2 Catalysts on H_3PO_4 Content[a]

molar ratio P/Zr	amount of DMC (mmol)	BET surface area (m^2/g)
0	0.08	118
0.0125	0.20	178
0.025	0.26	189
0.05	0.30	216
0.1	0.29	231
0.3	0.05	214
0.5	nd[b]	210
0.7	nd	94
1	nd	11

[a] Reaction conditions: CH_3OH/CO_2 = 192/200 mmol; catalyst weight, 0.5 g; reaction temperature, 403 K; reaction time, 2 h. [b] nd = not detected.

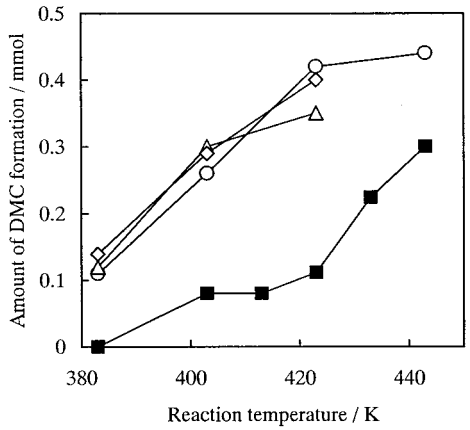

Figure 1. Dependence of DMC formation on the reaction temperature over ZrO_2 (■) and H_3PO_4/ZrO_2 [P/Zr = 0.025 (○), 0.05 (△), and 0.1 (◇)]. Reaction conditions: CH_3OH/CO_2 = 192/200 mmol; catalyst weight, 0.5 g; reaction time, 2 h.

NH_3-TPD profiles were obtained by a mass spectrometer (Balzers, Prisma QMS 200). The intensity of the mass signal (m/e = 16) was monitored. Sample pretreatment and gas adsorption were performed in a closed circulating vacuum system. Before the measurements of the TPD profiles, the sample was evacuated for 1 h at room temperature. The sample weight was 0.05 g. The heating rate was about 7 K/min.

Results and Discussion

DMC Synthesis from CH_3OH and CO_2. Table 1 shows the dependence of DMC formation and the BET surface area of H_3PO_4/ZrO_2 catalysts on the H_3PO_4 content. Both the amount of DMC formation and the BET surface area increased with increasing H_3PO_4 content at low P/Zr. The DMC amount reached a maximum at P/Zr = 0.05 and then decreased with increasing H_3PO_4 content. Furthermore, the surface area also increased with increasing H_3PO_4 content until P/Zr = 0.1 and then decreased. Although H_3PO_4/ZrO_2 (P/Zr = 0.3 and 0.5) had a high surface area, the activity of DMC formation was very low. This suggests that the DMC formation is not directly related to the surface area of H_3PO_4/ZrO_2 (Table 1).

Figure 1 shows the dependence of DMC formation on the reaction temperature over ZrO_2 and H_3PO_4/ZrO_2 (P/Zr = 0.025, 0.05, and 0.1). DMC formation with ZrO_2 is controlled by the reaction rate under these reaction conditions. Modification with H_3PO_4 enhanced the activity at all of the reaction temperatures. It seems that the amount of DMC formation on H_3PO_4/ZrO_2 (P/Zr = 0.025) at 443 K reached the equilibrium level. The DMC amount on H_3PO_4/ZrO_2 at 423 K became about 4 times larger than that on ZrO_2. The amount of DMC on H_3PO_4/ZrO_2

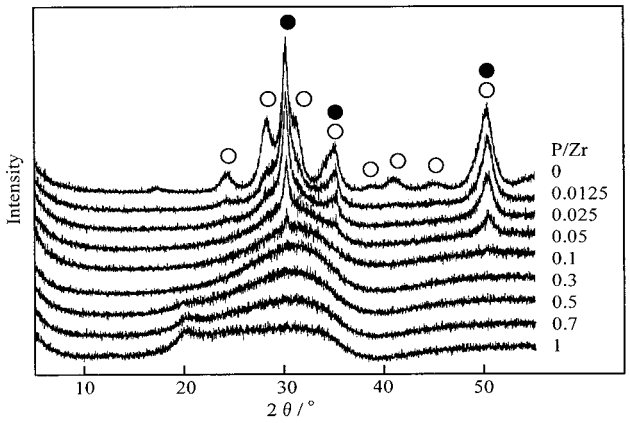

Figure 2. Cu Kα XRD patterns of fresh H_3PO_4/ZrO_2 catalysts with varying H_3PO_4 contents. Crystal structure: metastable tetragonal (●) and monoclinic (○).

at 403 K was comparable to that on ZrO_2 at 443 K. While DMC formation was not observed on ZrO_2 at 383 K, about 0.10 mmol of DMC was formed on H_3PO_4/ZrO_2. Besides, the amounts of DME and CO, which are expected byproducts, were also smaller than the detection limit of H_3PO_4/ZrO_2 under these reaction conditions. Therefore, the selectivity of DMC formation on H_3PO_4/ZrO_2 is estimated to be 100%. The amount of DMC formation on H_3PO_4/ZrO_2 (P/Zr = 0.05) at 383 K for 64 h was 0.53 mmol, where DME formation was not detected at all. The DME formation rate was found to be very low. By modification with H_3PO_4, the reaction temperature could be lowered by 40 K for the same level of DMC formation on ZrO_2.

We have calculated the equilibrium level of the CH_3OH conversion under our reaction conditions to be around 1% (DMC = ca. 0.96 mmol at 373−473 K). This value is higher than that of the experimental results, but this seems to be because our calculation did not consider H_2O as an impurity. Because the reactor, reactants, and catalyst surface should contain H_2O as an impurity, the amount is difficult to estimate. H_2O as an impurity may decrease the equilibrium level of DMC formation.[12]

Catalyst Characterization. XRD patterns of fresh H_3PO_4/ZrO_2 catalysts with various H_3PO_4 contents are shown in Figure 2. For ZrO_2, both the metastable-tetragonal and monoclinic phases were observed. The metastable-tetragonal phase gradually decreased and the monoclinic phase almost disappeared with the increasing content of H_3PO_4. The metastable-tetragonal phase was predominantly formed on H_3PO_4/ZrO_2 (P/Zr = 0.05), which exhibited the highest activity, as shown in Table 1. At P/Zr > 0.3, H_3PO_4/ZrO_2 catalysts did not show the diffraction patterns of either the metastable-tetragonal phase or the monoclinic phase. With a higher H_3PO_4 content, a new peak appeared around $2\theta = 20°$. This peak has not been identified, but it seems to be due to some salt compounds formed between the zirconium and phosphate ions.

Figure 3 shows the ^{31}P MAS NMR spectra of fresh H_3PO_4/ZrO_2 catalysts with various H_3PO_4 contents at room temperature. The broad peaks of each spectrum indicate that the phosphate species on H_3PO_4/ZrO_2 are not homogeneous. The peak at $\delta = -7.5$ ppm (P/Zr = 0.0125 in Figure 3) cannot be assigned at present. The broad peak at $\delta = -10.8$ ppm (P/Zr = 0.3 in Figure 3) is thought to be assigned to $(H_2PO_4)^-$, according to the report.[16] This suggests that the salt of the $(H_2PO_4)^-$ and zirconium ion is formed. The broad peaks around $\delta = -5.0$ ppm (P/Zr = 0.0125, 0.05, and 0.1 in Figure 3) are still ambiguous. These peaks around $\delta = -5.0$ ppm can be assigned

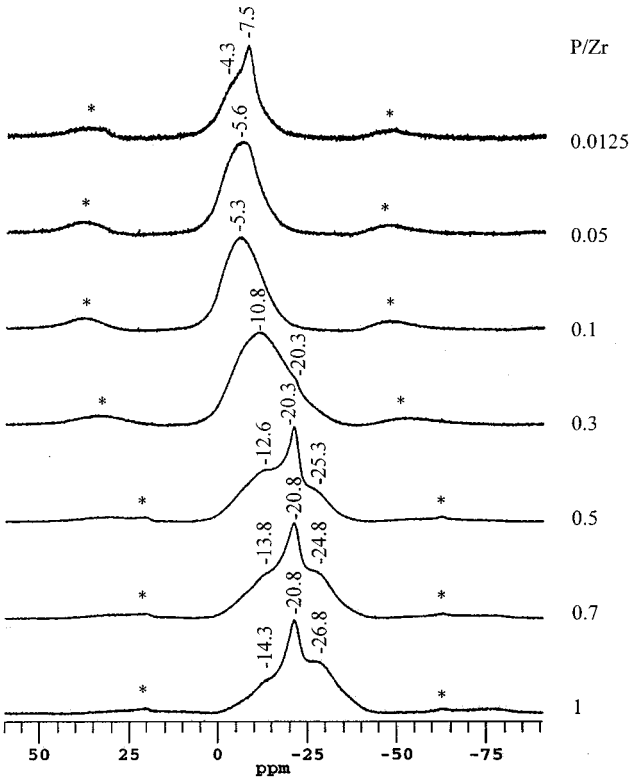

Figure 3. ^{31}P MAS NMR spectra of fresh H_3PO_4/ZrO_2 catalysts with varying H_3PO_4 contents at room temperature: (*) spinning sidebands; resonance frequency, 121.65 MHz; spinning rate, 5.0 kHz; pulse delay, 15 s and single pulse; reference signal, 85% H_3PO_4, $NH_4H_2PO_4$ (secondary standard).

to both the monophosphates (Q_0) and the end chain (Q_1) PO_4 groups of pyrophosphates.[17] In any case, these peaks are not due to the middle chain (Q_2) of polyphosphates.[18] This indicates that the dispersion of phosphate species on H_3PO_4/ZrO_2 (P/Zr = 0.0125, 0.05, and 0.1) is very high. The peaks around $\delta = -14$, -20 (major), and -25 ppm (P/Zr = 0.5−1 in Figure 3) seem to be due to the ^{31}P nuclei of the zirconium phosphates,[19] which indicate that some salt compounds of H_3PO_4/ZrO_2 (P/Zr = 0.5, 0.7, and 1.0) are formed. This is supported by the XRD patterns in Figure 2 as described previously. From these results, it is suggested that the most active species is the monophosphate or pyrophosphate and that the zirconium phosphates do not exhibit catalytic activity for DMC formation from CH_3OH and CO_2.

LRS spectra of fresh ZrO_2 and H_3PO_4/ZrO_2 catalysts are shown in Figure 4. It has been reported that the tetragonal phase ZrO_2 exhibits typical Raman bands at 148, 263, 325, 472, 608, and 640 cm^{-1} and that the monoclinic phase ZrO_2 exhibits bands at 140, 173, 185, 216, 260, 301, 328, 342, 378, 471, 499, 533, 553, 610, and 632 cm^{-1}.[20,21] For ZrO_2, the tetragonal phase seems to be the major phase from the XRD pattern in Figure 2, but the monoclinic phase seems to be the major phase from the LRS spectrum in Figure 4. Considering that LRS is the near-surface sensitive method, these results indicate that the phase composition on the surface is different from that in the bulk. A similar tendency has been reported previously.[20] On the other hand, all of the bands observed for H_3PO_4/ZrO_2 (P/Zr = 0.0125, 0.025, and 0.05) can be assigned to the tetragonal phase. By modification with H_3PO_4, the tetragonal phase was predominantly formed on the surface as well as in the bulk. We think that there is an interaction between the phosphate and the tetragonal zirconia. This is due to the result that the catalyst

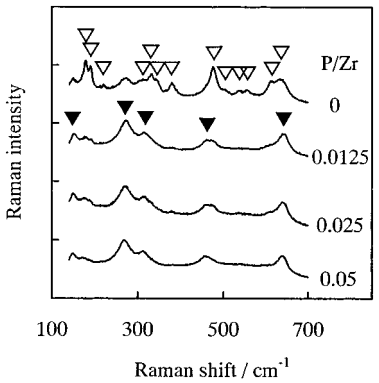

Figure 4. LRS spectra of fresh ZrO_2 and H_3PO_4/ZrO_2 (P/Zr = 0.0125, 0.025, and 0.05): Raman bands, metastable tetragonal (▼) and monoclinic (▽).

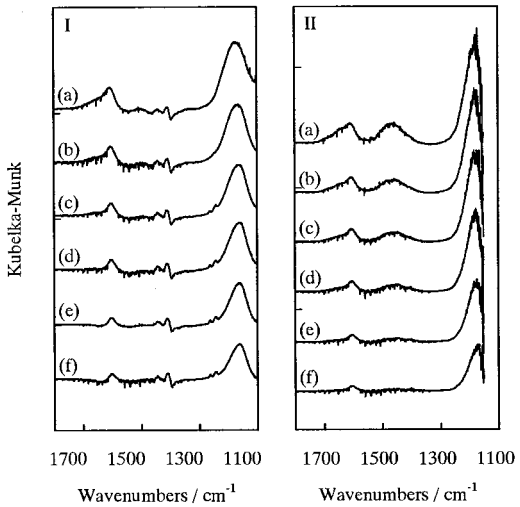

Figure 5. DRIFT spectra of NH_3 adsorbed on ZrO_2 (I) and H_3PO_4/ZrO_2 (P/Zr = 0.05) (II) at various temperatures: (a) at 293 K after adsorption, (b) after subsequent elevation of temperature to 373 K, (c) at 423 K, (d) at 473 K, (e) at 573 K, and (f) at 673 K (subtracted spectra). Pretreatment: 673 K for 0.5 h under N_2 flow.

prepared by the impregnation of H_3PO_4 on monoclinic zirconiashowed very low activity for DMC formation.[13] It is expected that H_3PO_4 can react with a basic hydroxide on monoclinic zirconia and form P−O−Zr (monoclinic); however, this is not effective for DMC formation. It is thought that surface-tetragonal zironia, which is stabilized by the addition of H_3PO_4, is very important for DMC synthesis.

Figure 5 shows the DRIFT spectra of NH_3 adsorbed on ZrO_2 and H_3PO_4/ZrO_2 (P/Zr = 0.05) under NH_3-TPD. When NH_3 was adsorbed at 298 K, both spectra (I and II in Figure 5) exhibited bands at 1605 and 1180−1160 cm^{-1}. These bands can be assigned to the asymmetric and symmetric bending modes of NH_3 coordinated to Lewis acid sites.[22] These intensities decreased with the temperature. Only the spectra of H_3PO_4/ZrO_2 (P/Zr = 0.05) (II in Figure 5) exhibit the band at 1470−1460 cm^{-1}. The band characteristic of the NH_4^+ ion is expected near 1450−1400 cm^{-1}, and the peak at the lower wavenumber generally corresponds to a stronger acid site.[23] In ionic solids (NH_4Cl, etc.), the asymmetric NH_4^+ bending wavenumber is near 1400 cm^{-1}, and the band is sharp. When the Brønsted acid site is weak such that proton transfer is less complete and the interaction is more of the type MO···H··· NH_3, the asymmetric deformation mode lies near 1450 cm^{-1}.[23] Therefore, the band at 1470−1460 cm^{-1} can be assigned to the asymmetric bending modes of NH_4^+ protonated from the

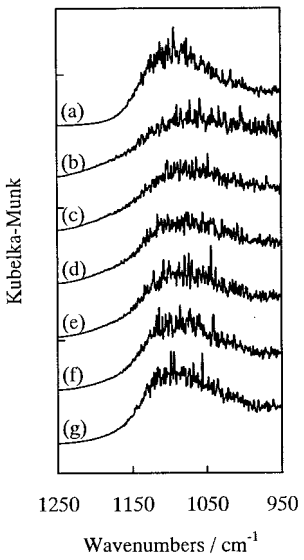

Figure 6. DRIFT spectra of NH_3 adsorbed on H_3PO_4/ZrO_2 (P/Zr = 0.05) at various temperatures: (a) at 293 K before adsorption, (b) at 293 K after adsorption, (c) after subsequent elevation of temperature to 373 K, (d) at 423 K, (e) at 473 K, (f) at 573 K, and (g) at 673 K. Pretreatment: 673 K for 0.5 h under N_2 flow.

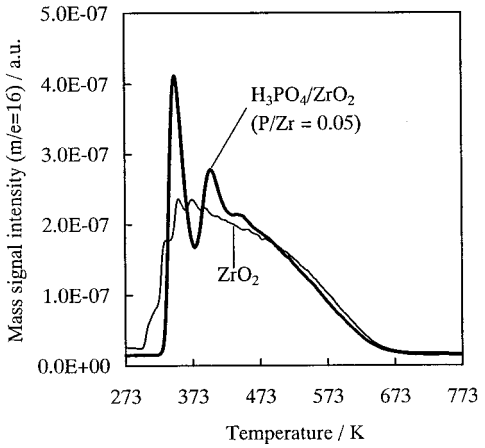

Figure 7. Profiles of TPD of NH_3 adsorbed on ZrO_2 (—) and H_3PO_4/ZrO_2 (P/Zr = 0.05) (—): NH_3 adsorption, P_{NH_3} = 6.6 kPa at 293 K; TPD conditions, heating rate of 7 K/min and sample weight of 0.05 g.

extremely weak Brønsted acid sites of the H_3PO_4/ZrO_2 (P/Zr = 0.05) surface. This band intensity decreased with the temperature and almost disappeared at 573 K, while the bands at 1605 and 1180−1160 cm^{-1} were present even at 673 K. These results indicate that Lewis acid sites are present on both ZrO_2 and H_3PO_4/ZrO_2 (P/Zr = 0.05) while the weak Brønsted acid sites are present on H_3PO_4/ZrO_2 (P/Zr = 0.05).

As shown in Figure 6, the NH_3 band at 1100 cm^{-1} shifted to lower wavenumbers. This band can be assigned to P−O stretching modes.[24] As the temperature was increased and NH_3 was desorbed, this shift became smaller and almost recovered at 573 K. This behavior due to temperature seems to be correlated with that of the intensity of the band at 1470−1460 cm^{-1} (see II in Figure 5), which indicates the presence of weak Brønsted acid sites on H_3PO_4/ZrO_2 (P/Zr = 0.05). Hence, it is suggested that the weak Brønsted acid sites on H_3PO_4/ZrO_2 (P/Zr = 0.05) are located near the P atoms.

Figure 7 shows the TPD profiles of NH_3 adsorbed on ZrO_2 and H_3PO_4/ZrO_2 (P/Zr = 0.05). NH_3 was desorbed in a wide temperature range. On average, a larger desorption amount of NH_3 on H_3PO_4/ZrO_2 (P/Zr = 0.05) than that on ZrO_2 was

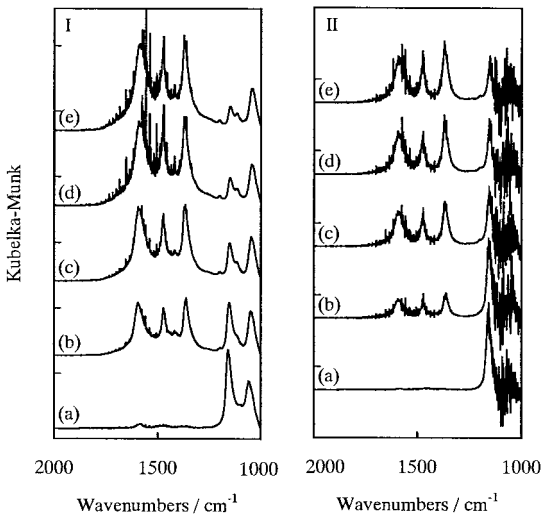

Figure 8. DRIFT spectra of CH_3OH adsorption and successive CO_2 introduction at 443 K on ZrO_2 (I) and H_3PO_4/ZrO_2 (P/Zr = 0.05) (II): (a) after CH_3OH adsorption, (b) after CO_2 introduction under 0.1 MPa, (c) at 1.0 MPa, (d) at 3.0 MPa, and (e) at 5.0 MPa (subtracted spectra). Pretreatment: 673 K for 0.5 h under N_2 flow.

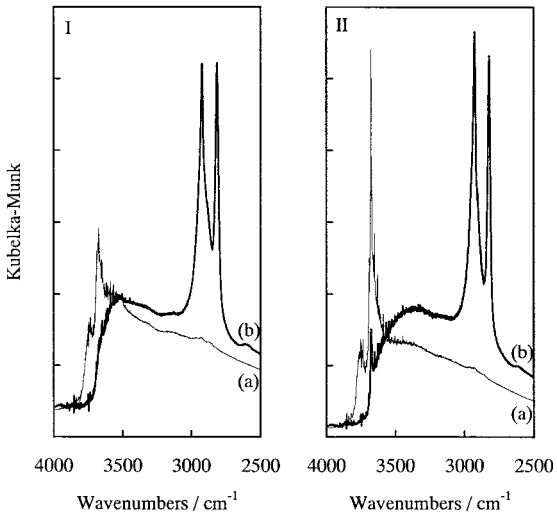

Figure 9. DRIFT spectra of surface hydroxyl groups of ZrO_2 (I) and H_3PO_4/ZrO_2 (P/Zr = 0.05) (II) before and after CH_3OH adsorption at 443 K: (a) before CH_3OH adsorption (—) and (b) after CH_3OH adsorption (—). Pretreatment: 673 K for 0.5 h under N_2 flow.

observed in the lower-temperature range. This indicates that the modification of ZrO_2 with H_3PO_4 led to an increase in the number of weaker acid sites. These acid sites on H_3PO_4/ZrO_2 (P/Zr = 0.05) can be attributed to the weak Brønsted acid sites near the P atoms, which do not exist on ZrO_2, as described previously.

Figure 8 shows the DRIFT spectra of CH_3OH adsorption and successive CO_2 introduction at 443 K on ZrO_2 and H_3PO_4/ZrO_2 (P/Zr = 0.05). No significant differences between the two series of spectra are observed. CH_3OH adsorption led to the appearance of the bands at 1160 and 1054 cm^{-1}. These can be assigned to the C−O stretching modes of terminal (t-OCH_3) and bridged (b-OCH_3) methoxy species, respectively.[25] When CO_2 was introduced to the CH_3OH-preadsorbed catalysts, the band intensity at 1160 cm^{-1} decreased and the bands at 1600, 1474, 1370, and 1130 cm^{-1} appeared. The intensity of these bands increased with the increase in CO_2 pressure. These bands can be assigned to the methyl carbonate-like species.[25] CO_2 introduction did not affect the band at 1054 cm^{-1} assigned to b-OCH_3. These results indicate that the methyl carbonate species is easily formed from the interaction between CO_2 and t-OCH_3 and that the formation is more favorable under higher CO_2 pressure. This coincides with the dependence of CO_2 pressure on the DMC formation amount, which has been reported on ZrO_2 before.[14]

Figure 9 shows the DRIFT spectra of the surface hydroxyl groups of ZrO_2 and H_3PO_4/ZrO_2 (P/Zr = 0.05) before and after CH_3OH adsorption at 443 K. Before CH_3OH adsorption, the bands at 3750 and 3680 cm^{-1} were observed on both of the catalysts. These bands can be assigned to the O−H stretching modes of terminal (t-OH) and bridged (b-OH) hydroxyl groups, respectively.[25] After CH_3OH adsorption, neither t-OH nor b-OH on ZrO_2 was observed (I in Figure 9). On the other hand, b-OH on H_3PO_4/ZrO_2 (P/Zr = 0.05) was still present with significant intensity, though t-OH disappeared (II in Figure 9). It seems that the rest of the b-OH on H_3PO_4/ZrO_2 (P/Zr = 0.05) after CH_3OH adsorption corresponds to the weak Brønsted acid sites near the P atoms, which is indicated by FTIR spectra of NH_3 adsorption and NH_3-TPD profiles. From these results, the modification of ZrO_2 with phosphate forms the weak and bridged Brønsted acid sites. In this case, the direct interaction

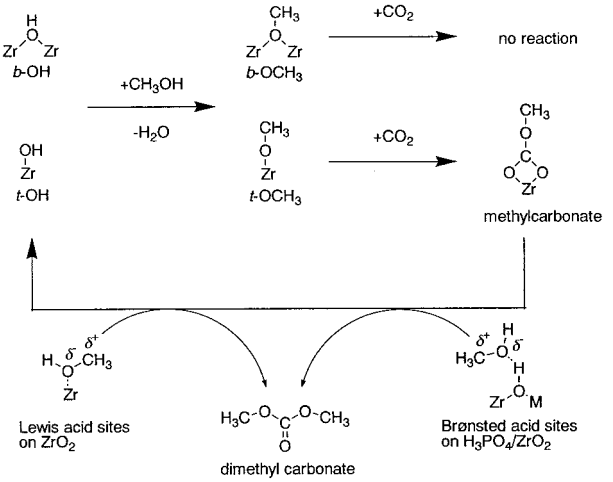

Figure 10. Model of mechanism for DMC synthesis from CH_3OH and CO_2 on ZrO_2 and H_3PO_4/ZrO_2 (P/Zr = 0.05): M = P or Zr induced by adjacent phosphoric species.

between Zr (tetragonal) and P is essential to effective acid formation. At present, the weak and bridged Brønsted acid sites are thought to be on the bridging oxide ion in P−O−Zr (tetragonal) or Zr−O−Zr (−O−P), which is influenced by the interaction with phosphate.

CH_3OH adsorption led to the appearance of the bands at 2924 and 2820 cm^{-1} on both of the catalysts. These bands can be assigned to the C−H stretching modes of t- and b-OCH_3 species, respectively.[25]

From the previous results on ZrO_2 catalysts,[12,14] it is suggested that acid−base bifunction is the key to selective DMC formation. The methyl carbonate species is considered to be the reaction intermediate. In this case, DMC is formed from the methyl carbonate species and the methyl cation, which is related to the activation of CH_3OH on the acid sites. The reaction scheme of DMC synthesis from CH_3OH and CO_2 can be postulated as shown in Figure 10 and described as follows.

(I) For CH_3OH activation on base sites, t- and b-OH are converted to t- and b-OCH_3 when CH_3OH is adsorbed.

(II) For CO_2 activation on base sites, t-OCH_3 reacts with CO_2 to form methyl carbonate, and b-OCH_3 cannot react.

(III) For CH_3OH activation on acid sites, DMC is formed from the reaction between methyl carbonate and the methyl cation.

It is suggested that the high selectivity of DMC formation on ZrO_2 and H_3PO_4/ZrO_2 (P/Zr = 0.05) is due to the rapid conversion of t-OCH_3 to the methyl carbonate species under high CO_2 pressure, which could be observed by DRIFT. Step III, which is related to the activation of CH_3OH on acid sites, may be the rate-determining step in DMC formation. Brønsted acid sites on H_3PO_4/ZrO_2 (P/Zr = 0.05) seem to be more favorable than Lewis acid sites on ZrO_2 for the CH_3OH activation step III. This can explain the promotion of catalytic activity for DMC formation by modification of ZrO_2 with H_3PO_4.

Conclusions

(1) Modification of ZrO_2 with H_3PO_4 enhanced the activity for DMC synthesis remarkably, especially at low temperatures.

(2) The optimum composition of H_3PO_4/ZrO_2 is P/Zr = 0.025−0.1.

(3) Both ZrO_2 and H_3PO_4/ZrO_2 (P/Zr = 0.05) had Lewis acid sites, though only H_3PO_4/ZrO_2 (P/Zr = 0.05) had weak Brønsted acid sites. The direct interaction between Zr (tetragonal) and P is essential to the formation of weak Brønsted acid sites.

(4) When CO_2 was introduced to the CH_3OH-preadsorbed catalysts, only t-OCH_3 was decreased and the methyl carbonate species was formed. The methyl carbonate species can be the reaction intermediate of DMC formation from CH_3OH and CO_2.

(5) Brønsted acid sites on H_3PO_4/ZrO_2 (P/Zr = 0.05) can be more effective than Lewis acid sites on ZrO_2 for CH_3OH activation on the acid sites. The reaction between the activated CH_3OH on the acid sites and the methyl carbonate species gives DMC.

(6) Acid−base bifunctional catalysis is essential in selective DMC synthesis from CH_3OH and CO_2.

References and Notes

(1) Aresta, M.; Quaranta, E. *CHEMTECH* **1997**, 32−40.

(2) Ono, Y. *Appl. Catal., A* **1997**, *155*, 133−166.

(3) Pacheco, M. A.; Marshall, C. L. *Energy Fuels* **1997**, *11*, 2−29.

(4) Shaikh, A.-A. G.; Sivaram, S. *Chem. Rev.* **1996**, *96*, 951−976.

(5) Romano, U.; Tesei, R.; Mauri, M. M.; Rebora, P. *Ind. Eng. Chem. Prod. Res. Dev.* **1980**, *19*, 396−403.

(6) Molzahn, D.; Jones, M. E.; Hartwell, G. E.; Puga, J. U.S. Patent 5,387,708, 1995.

(7) King, S. S. T.; Jones, M. E.; Olken, M. M. U.S. Patent 5,391,803, 1995.

(8) Matsuzaki, T.; Nakamura, A. *Catal. Surv. Jpn.* **1997**, *1*, 77−88.

(9) Sakakura, T.; Saito, Y.; Okano, M.; Choi, J.-C.; Sako, T. *J. Org. Chem.* **1998**, *63*, 7095−7096.

(10) Sakai, S.; Fujinami, T.; Yamada, T.; Furusawa, S. *Nippon Kagaku Kaishi* **1975**, *10*, 1789−1794.

(11) Kizlink, J.; Pastucha, I. *Collect. Czech. Chem. Commun.* **1995**, *60*, 687−692.

(12) Tomishige, K.; Sakaihori, T.; Ikeda, Y.; Fujimoto, K. *Catal. Lett.* **1999**, *58*, 225−229.

(13) Ikeda, Y.; Furusawa, Y.; Tomishige, K.; Fujimoto, K. *ACS Symp. Ser.* **2001**, in press.

(14) Tomishige, K.; Ikeda, Y.; Sakaihori, T.; Fujimoto, K. *J. Catal.* **2000**, *192*, 355−362.

(15) Ikeda, Y.; Sakaihori, T.; Tomishige, K.; Fujimoto, K. *Catal. Lett.* **2000**, *66*, 59−62.

(16) Kaneno, M.; Yamaguchi, S.; Nakayama, H.; Miyakubo, K.; Ueda, T.; Eguchi, T.; Nakamura, N. *Int. J. Inorg. Mater.* **1999**, *1*, 379−384.

(17) Caro, J.; Bülow, M.; Derewinski, M.; Haber, J.; Hunger, M.; Kärger, J.; Pfeifer, H.; Storek, W.; Zibrowius, B. *J. Catal.* **1990**, *124*, 367−375.

(18) Segawa, K.; Nakajima, Y.; Nakata, S.; Asaoka, S.; Takahashi, H. *J. Catal.* **1986**, *101*, 81−89.

(19) Hayashi, S.; Hayamizu, K. *Bull. Chem. Soc. Jpn.* **1989**, *62*, 3061−3068.

(20) Yamamoto, T.; Tanaka, T.; Takenaka, S.; Yoshida, S.; Onari, T.; Takahashi, Y.; Kosaka, T.; Hasegawa, S.; Kudo, M. *J. Phys. Chem. B* **1999**, *103*, 2385−2393.

(21) Mercera, P. D. L.; van Ommen, J. G.; Doesburg, E. B. M.; Burggraaf, A. J.; Ross, J. R. H. *Appl. Catal.* **1990**, *57*, 127−148.

(22) Yamaguchi, T.; Nakano, Y.; Tanabe, K. *Bull. Chem. Soc. Jpn.* **1978**, *51*, 2482−2487.

(23) Dang, Z.; Anderson, B. G.; Amenomiya, Y.; Morrow, B. A. *J. Phys. Chem.* **1995**, *99*, 14437−14443.

(24) Nakamoto, K. *Infrared Spectra of Inorganic and Coordination Complexes*; Wiley-Interscience: New York, 1970; p 117.

(25) Bensitel, M.; Moravek, V.; Lamotte, J.; Sauer, O.; Lavalley, J.-C. *Spectrochim. Acta* **1987**, *43A*, 1487−1491.